Theoretical prediction of the antiferromagnetic ground state of a C defect on Si(001)

Jin-Ho Choi and Jun-Hyung Cho*
Department of Physics, Hanyang University, 17 Haengdang-Dong, Seongdong-Ku, Seoul 133-791, Korea
(Received 19 June 2009; revised manuscript received 17 August 2009; published 17 September 2009)

We have performed first-principles density-functional calculations for the C defect on Si(001), which has been experimentally identified in terms of the dissociative adsorption of a single water molecule on two adjacent dimers. Unlike the hitherto accepted nonmagnetic structure that involves the buckling of two Si dangling bonds (DBs) within the C defect, the presently proposed structure shows that the two DBs are antiferromagnetically coupled with each other, thereby giving rise to a suppression of their buckling. This antiferromagnetic ground state of C defect reproduces the key features observed in the STM and STS experiments.

DOI: 10.1103/PhysRevB.80.125314 PACS number(s): 73.20.At, 71.28.+d, 71.55.−i

The Si(001) surface is one of the most investigated substrates because of its technological importance in the fabrication of nanoelectronic devices[1,2] as well as for various fundamental issues such as chemical reaction,[3,4] surface dynamics,[5] and thin-film growth.[6] This surface is atomically reconstructed with dimerization,[7] thereby removing one of the two dangling bonds (DBs) associated with each atom on the bulk-truncated surface. Since such a dimerization of surface Si atoms induces a stress on Si(001), there exist a number of atomic-scale defects to relieve the surface stress.[8–15] These defects play an important role in the adsorption, diffusion, and clustering of mobile atoms or molecules on the surface.[5,16] Thus, a detailed understanding of the defect structures is prerequisite to utilizing the Si(001) surface as a template for the formation of nanoengineered functional materials. The scanning tunneling microscopy (STM) measurements of a clean Si(001) surface showed certain amounts of defects.[8–10] Hamers and Köhler[8] classified the observed defects into three types (i.e., *A*-, *B*-, and *C*-type defects). While the *A*- and *B*-type defects were earlier identified as one and two-dimer vacancies, respectively,[14,15] the *C*-type defect was recently disclosed to be due to the dissociative adsorption of a single water molecule on the same side of two adjacent Si dimers (see Fig. 1).[11–13]

The STM studies[9–12] showed that the *C* defect appears as two protrusions on one side of two adjacent Si dimers and depression on the other side. In the empty-state (filled-state) STM image, the two protrusions were observed to be brighter (darker) than the neighboring dimers.[10,11] Here, the sizes of two protrusions in the empty-state image are different from each other, apparently looking like an asymmetric teardrop-shaped protrusion. Using scanning tunneling spectroscopy (STS), Hata *et al.*[10] found that at room temperature all of the *C* defects are metallic, but as temperature is lowered to 80 K, some of them undergo a transition from metallic to semiconducting. Especially, the STS spectra of the semiconducting *C* defect showed that the $(dI/dV)(I/V)$ versus V curves taken at different positions on top of the *C* defect are highly symmetric regarding the plane bisecting the *C* defect perpendicular to the dimer row direction. On the theoretical side, there are a few first-principles investigations for the C defect,[12,13] all of which were based on the *nonmagnetic* (NM) structural model. As discussed below, this NM structure that involves the buckling of two DBs within the C defect [see Fig. 1(a)] fails to reproduce the key features observed in the STM and STS measurements. Thus, despite the experimental evidence that the *C* defect originates from the dissociative adsorption of a single water molecule, its structural model still remains unsettled.

In this paper, we theoretically predict a new structural model for the C defect, where two adjacent DBs are antiferromagnetically coupled with each other. This antiferromagnetic (AF) ordering caused by highly correlated DB electrons is found to be energetically favored over the Jahn-Teller-like distortion involved in the NM structural model. The proposed AF configuration in which the buckling of two DBs is almost suppressed not only reproduces the observed features in the STM data,[11] but also gives a highly symmetric feature of the local density of states (LDOS) with respect to the [110] plane bisecting the C defect, fully compatible with the observed STS spectra.[10]

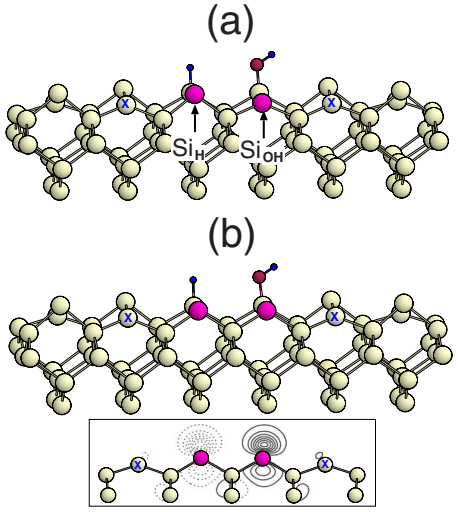

FIG. 1. (Color online) Optimized structure of the C defect within the (a) NM and (b) AF configurations. The circles represent Si, O, and H atoms with decreasing size. The two Si atoms containing a single DB are designated as Si_H and Si_{OH}. The down Si atoms of neighboring dimers are marked X. The spin density $n_\uparrow(\mathbf{r}) - n_\downarrow(\mathbf{r})$ for the AF configuration is also given in the inset of (b). The contour plots are drawn in the vertical plane containing the Si_H and Si_{OH} atoms. The first solid (dashed) line is at 0.01 (−0.01) electrons/Å^3 with spacings of 0.02 (−0.02) electron/Å^3.

TABLE I. Calculated energies of the NM, FM, and AF configurations. The energy of the NM configuration is set to zero. For each configuration, the band gap at the Y point (see Fig. 2) is also given. The values in parentheses denote the calculated ones for another NM structure obtained by Okano and Oshiyama (Ref. 13).

	ΔE (meV)	E_{gap} (meV)
NM	0 (35)	488 (408)
FM	13	378
AF	−72	698

The total-energy and force calculations were performed using spin-polarized density-functional theory[17] (DFT) within the generalized-gradient approximation.[18] The Si and H (O) atoms are described by norm-conserving[19] (ultrasoft[20]) pseudopotentials. The surface was modeled by the periodic slab geometry. Each slab contains six Si atomic layers, and the bottom Si layer is passivated by two H atoms per Si atom. The theoretical equilibrium lattice constant amounts to 5.48 Å. The vacuum spacing between these slabs is about 12 Å. The electronic wave functions were expanded in a plane-wave basis set with a cutoff of 25 Ry, and the electron density was obtained from the wave functions at eight **k** points in the surface Brillouin zone of the 2×5 unit cell. All the atoms except the bottom two Si layer were allowed to relax along the calculated Hellmann-Feynman forces until all the residual forces components were less than 1 mRy/bohr. Our calculation scheme has been successfully applied for the adsorption of various molecules on Si(001).[21]

All previous DFT calculations[12,13] for the C defect were performed with the NM structural model. However, we here extend the previous work by taking spin polarization of electrons into account. According to the STM data of Hata *et al.*,[10] the semiconducting C defect observed at low temperatures below 80 K disturbs the ordering of the surrounding buckled dimers, yielding a separation of $p(2\times2)$ and $c(4\times2)$ domains. Therefore, the down-buckled side (marked X in Fig. 1) of neighboring Si dimers are located on both sides of the Si_H and Si_{OH} atoms. To simulate such an ordering of neighboring dimers, we employed a 2×5 unit cell[22] that involved five dimers along the dimer row. We optimized the atomic structure within the NM, ferromagnetic (FM), and AF configurations. The calculated total energies of various configurations are given in Table I. We find that the AF (FM) configuration is more (less) stable than the NM configuration by about 72 (13) meV. Thus, the ground state of the C defect is not NM, but is AF.[23]

From the energy difference between the FM and AF configurations, we estimate the exchange coupling constant between two spins as 85 meV.[24] The total spin of the AF configuration is zero, while that of the FM configuration is $2\mu_B$ (i.e., $1\mu_B$ per dangling bond). The calculated spin density $n_\uparrow(\mathbf{r})-n_\downarrow(\mathbf{r})$ for the AF configuration is shown in Fig. 1(b). We note that the spin density overlaps between Si_H and Si_{OH} through the subsurface atoms. Therefore, the AF coupling between two spins is likely to be driven by a superexchange interaction[25] via the bridging covalent-bonded subsurface Si atoms.

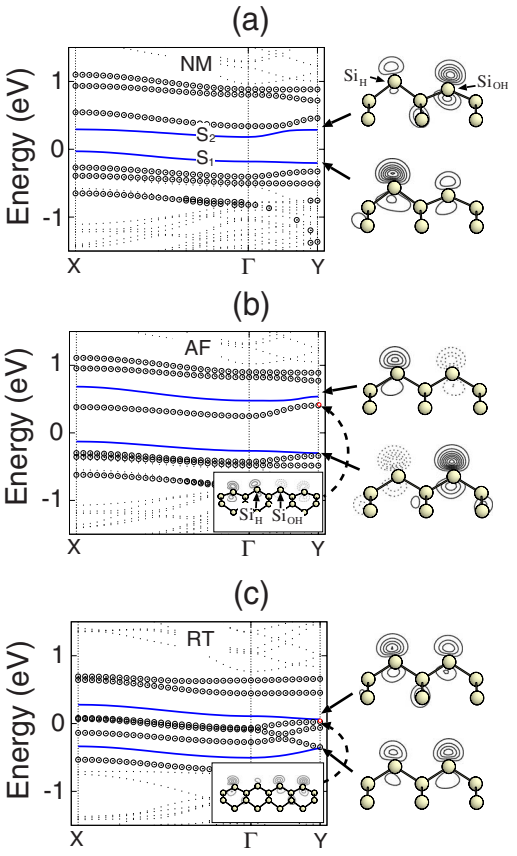

FIG. 2. (Color online) Calculated band structures for the (a) NM, (b) AF, and (c) room-temperature (see the text) configurations. The energy zero represents the Fermi level. The direction of the Γ-X(Y) line is perpendicular (parallel) to the Si dimer row. Open circles represent the states containing more than 50% of charge in the three bare Si dimers. The charge characters of DB states (S_1 and S_2) at the Y point are also shown. The insets in (b) and (c) show charge characters of a surface state, which shows a hybridization between the DBs and neighboring dimers. For the AF configuration, the solid (dashed) line represents the positive (negative) spin density. In the contour plot, a uniform increment of 0.01 electrons/Å^3 is used.

The optimized structures of the NM and AF configurations are shown in Figs. 1(a) and 1(b), respectively. In the NM configuration, the Si_H and Si_{OH} atoms are displaced up and down, respectively, yielding a height difference (Δh) of 0.54 Å. On the other hand, in both the AF and FM configurations, the buckling of the Si_H and Si_{OH} atoms is suppressed to be $\Delta h=0.02$ Å, as a consequence of spin polarization. We note that the large height difference of Si_H and Si_{OH} in the NM configuration contradicts with the structure obtained by a previous DFT calculation of Okano and Oshiyama,[13] where Δh is only 0.05 Å. We find, however, that the latter NM structure is found to be less stable than the former NM one by 35 meV (see Table I).

Figures 2(a) and 2(b) show the calculated band structures for the NM and AF configurations of the C defect, respectively. We find two surface-state bands (designated as S_1 and S_2) near the Fermi level, which originate from two DBs within the C defect. For the AF configuration, the energy difference between the S_1 and S_2 bands is 835 meV at the Y

point. Note that there is an additional empty state between the S_1 and S_2 bands [see Fig. 2(b)]. Therefore, the band gap of the AF configuration is 698 meV at the Y point, significantly larger than that (488 meV) of the NM configuration. This result indicates that the electronic energy gain obtained by spontaneous spin polarization is much greater than that obtained by a Jahn-Teller-like lattice distortion in the NM configuration. We note that the band gap in the highly buckled NM structure increases by 80 meV relative to the nearly nonbuckled NM one obtained by Okano and Oshiyama[13] (see Table I). This increase is caused by a rehybridization of the dangling orbitals, accompanied by a charge transfer from the down (Si_{OH}) to the up (Si_H) atom. As shown in Fig. 2(a), the charge characters of the S_1 and S_2 states reveal that these states represent DBs, which are localized at the Si_H and Si_{OH} atoms, respectively. In the AF configuration, the charge characters of the S_1 and S_2 states [see Fig. 2(b)] show the opposite separations of DB spins at the Si_H and Si_{OH} atoms. Note that the charge character of the surface state between the S_1 and S_2 bands reveals a weakly hybridization of the dangling orbitals of neighboring dimers with those of the Si_H and Si_{OH} atoms [see Fig. 2(b)].

The existence of the AF ordering within C defect reflects a strong electron-electron interaction due to the localized nature of DBs. In order to estimate the strength of repulsion between two DB electrons within the C defect, we evaluate the Hubbard correlation energy U by using the constrained DFT calculations.[26] Here, we simulate one electron transfer between the two DBs and calculate the change in the total energy. In the AF configuration, we obtain $U=1.55$ eV. This value is significantly larger than the electron transfer $t=0.17$ eV, which is estimated from the bandwidth of the S_1 state. If we assume that the two DBs are perfectly confined within the C defect, the exact diagonalization of Hubbard Hamiltonian[27] with those U and t gives rise to an AF ground state.

In the STM experiments,[9–12] the *C* defect was imaged as two protrusions on one side (containing the Si_H and Si_{OH} atoms) of two adjacent Si dimers and depression on the other side. In the observed empty-state (filled-state) STM image of C defect, the Si_H and Si_{OH} atoms appear brighter (darker) than the surrounding Si dimers. For comparison with the STM measurements, we simulate the constant-current STM images for the empty and filled states of NM and AF configurations using the Tersoff-Hamann approximation.[28] The results are displayed in Fig. 3, together with their cross-sectional views. We find that the empty-state images of the NM and AF configurations are similar to each other, showing an asymmetric teardrop-shaped protrusion. Their cross-sectional views along the line containing the Si_H and Si_{OH} atoms show that the peak heights of two protrusions are larger than those of neighboring dimers. For the filled-state image, we find a conspicuous difference between the NM and AF configurations, i.e., NM has a single bright protrusion at Si_H [see Fig. 3(a)], while AF shows two equally bright protrusions at both Si_H and Si_{OH} [see Fig. 3(b)]. From their cross-sectional views, it is seen that the peak height of the single protrusion in NM is nearly equal to those of neighboring dimers, while the two protrusions in AF are 0.49 Å lower in height than those of neighboring dimers. From our simulated STM images, we can say that the AF configuration reproduces the features observed in the STM measurements,[9,11,12] such as peak shape as well as peak brightness.

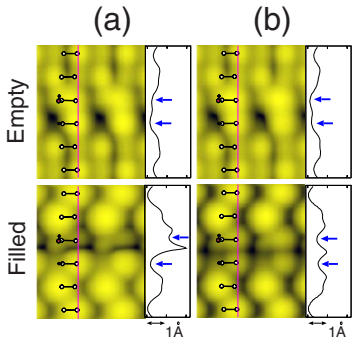

FIG. 3. (Color online) Simulated STM images within the (a) NM and (b) AF configurations, including the cross-sectional view along the line connecting the Si_H or Si_{OH} atoms. All the empty-state images are obtained by integrating the charge from E_F to $E_F+1.0$ eV, whereas the filled-state images are obtained from $E_F-1.0$ eV to E_F. All the images were taken at 6.7×10^{-6} electrons/Å^3. The arrows indicate the positions of Si_H and Si_{OH} atoms.

In their STS spectra from the semiconducting C defect, Hata *et al.*[10] observed two peaks P_1 and P_2 near the Fermi level (E_F), where P_1 is located at 0.35 eV below E_F and P_2 is located at 0.45 eV above E_F.[29] Here, the peak intensity of P_1 was measured to be $1.5\sim2$ times larger than that of P_2. Especially, the STS data taken at different lateral separations from the center of the C defect showed a highly symmetric feature with respect to the [110] plane bisecting the *C* defect. To examine these observed features of C defect, we calculate the LDOS inside the muffin-tin spheres centered at the Si_H and Si_{OH} atoms. The results for the NM and AF configurations are displayed in Figs. 4(a) and 4(b), respectively. In the NM configuration, the LDOS at Si_H and Si_{OH} show the ex-

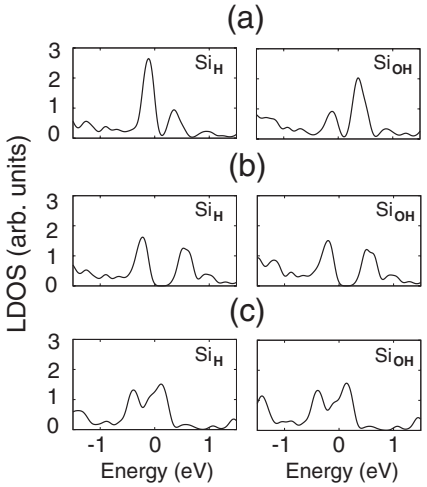

FIG. 4. Calculated local density of states within the muffin-tin spheres (whose radius was chosen as 1.2 Å) centered at the Si_H or Si_{OH} atoms: (a) the NM, (b) AF, and (c) room-temperature configurations.

istence of two peaks, but their patterns are totally different from each other [see Fig. 4(a)], that is, the highest peak at Si_H (Si_{OH}) appears below (above) E_F, reflecting the charge transfer from Si_{OH} to Si_H. On the other hand, in the AF configuration, the LDOS at Si_H and Si_{OH} are similar to each other [see Fig. 4(b)], showing that the highest peak is located around 0.24 eV below E_F and its intensity is ~1.2 times larger than that of the other peak located around 0.51 eV above E_F. Thus, unlike the case of the NM configuration, the AF configuration reproduces the features observed in the STS measurements such as the positions and intensities of two peaks as well as the above-mentioned highly symmetric feature of spectra on both sides of C defect.

Finally, we examine the observed metallic feature of C defect at room temperature by taking thermal activated flipping motion of buckled Si dimers into account.[30] It is well known that at room temperature, the observed symmetric-dimer STM images of Si(001) are ascribed to a dynamic flip-flop motion of buckled dimers.[31] We here simulate the room-temperature configuration of C defect with the symmetric-dimer model, where each bare Si dimer within the 2×5 unit cell is constrained to be symmetric. Here, we optimize the height as well as the bond length of each Si dimer within the symmetric-dimer model. The electronic band structure for such a room-temperature configuration is plotted in Fig. 2(c). We find the presence of three bands between the S_1 and S_2 bands, two of which cross E_F, thereby showing a metallic feature as observed[10] in the STS experiment. The charge character of such a surface state, shown in Fig. 2(c), exhibits some hybridization of the dangling orbitals of neighboring dimers with those of Si_H and Si_{OH}. Especially, the calculated LDOS [see Fig. 4(c)] shows that the peak above E_F has a slightly greater intensity compared to that below E_F, consistent with the STS data of Hata *et al.*[10]

In summary, our spin-polarized DFT calculations predict the AF ground state for the C defect on Si(001), where the two DBs generated by the dissociative adsorption of a single water molecule on two adjacent dimers are antiferromagnetically coupled with each other. Contrasting with the hitherto accepted NM structure for the C defect, the geometrical and electronic properties of the AF ground state are shown to be fully compatible with the STM and STS data.

This work was supported by Basic Science Research Program through the National Research Foundation of Korea (NRF) grant funded by the Ministry of Education, Science and Technology (Quantum Photonic Science Research Center).

*Corresponding author; chojh@hanyang.ac.kr

[1] J. T. Yates, Jr., Science **279**, 335 (1998).
[2] G. P. Lopinski, D. D. M. Wayner, and R. A. Wolkow, Nature (London) **406**, 48 (2000).
[3] C.-H. Chung, W.-J. Jung, and I.-W. Lyo, Phys. Rev. Lett. **97**, 116102 (2006).
[4] Y.-S. Kim, J.-Y. Koo, and H. Kim, Phys. Rev. Lett. **100**, 256105 (2008).
[5] M. McEllistrem, M. Allgeier, and J. J. Boland, Science **279**, 545 (1998).
[6] H. Wu, M. Hortamani, P. Kratzer, and M. Scheffler, Phys. Rev. Lett. **92**, 237202 (2004).
[7] R. Schlier and H. Fransworth, J. Chem. Phys. **30**, 917 (1959).
[8] R. J. Hamers and U. K. Köhler, J. Vac. Sci. Technol. A **7**, 2854 (1989).
[9] Z. Zhang, M. A. Kulakov, and B. Bullemer, Surf. Sci. **369**, L131 (1996).
[10] K. Hata, S. Ozawa, Y. Sainoo, K. Miyake, and H. Shigekawa, Surf. Sci. **447**, 156 (2000).
[11] M. Z. Hossain, Y. Yamashita, K. Mukai, and J. Yoshinobu, Phys. Rev. B **67**, 153307 (2003).
[12] S. Y. Yu, H. Kim, and J.-Y. Koo, Phys. Rev. Lett. **100**, 036107 (2008).
[13] S. Okano and A. Oshiyama, Surf. Sci. **554**, 272 (2004).
[14] J. Wang, T. A. Arias, and J. D. Joannopoulos, Phys. Rev. B **47**, 10497 (1993).
[15] S. R. Schofield, N. J. Curson, J. L. OBrien, M. Y. Simmons, R. G. Clark, N. A. Marks, H. F. Wilson, G. W. Brown, and M. E. Hawley, Phys. Rev. B **69**, 085312 (2004).
[16] Ph. Avouris and D. Cahill, Ultramicroscopy **42-44**, 838 (1992).
[17] P. Hohenberg and W. Kohn, Phys. Rev. **136**, B864 (1964); W. Kohn and L. Sham, *ibid.* **140**, A1133 (1965).
[18] J. P. Perdew, K. Burke, and M. Ernzerhof, Phys. Rev. Lett. **77**, 3865 (1996); **78**, 1396(E) (1997).
[19] N. Troullier and J. L. Martins, Phys. Rev. B **43**, 1993 (1991).
[20] D. Vanderbilt, Phys. Rev. B **41**, 7892 (1990); K. Laasonen, A. Pasquarello, R. Car, C. Lee, and D. Vanderbilt, *ibid.* **47**, 10142 (1993).
[21] J.-H. Cho, D. H. Oh, and L. Kleinman, Phys. Rev. B **65**, 081310(R) (2002); J.-H. Choi and J.-H. Cho, J. Am. Chem. Soc. **128**, 3890 (2006); J.-H. Choi and J.-H. Cho, Phys. Rev. Lett. **98**, 246101 (2007).
[22] We used a 2×5 unit cell rather than a 4×5 unit cell because the latter one cannot simulate the structure of alternating buckled dimers along the neighboring Si dimer row of the C defect (see Ref. 13).
[23] The dissociative adsorption of an H_2 molecule on two adjacent dimers also gives an AF ground state: see J. Y. Lee, J.-H. Choi, and J.-H. Cho, Phys. Rev. B **78**, 081303(R) (2008).
[24] L. Noodleman, J. Chem. Phys. **74**, 5737 (1981).
[25] P. W. Anderson, Phys. Rev. **79**, 350 (1950).
[26] V. I. Anisimov, I. V. Solovyev, M. A. Korotin, M. T. Czyżyk, and G. A. Sawatzky, Phys. Rev. B **48**, 16929 (1993).
[27] B. Alvarez-Fernández and J. A. Blanco, Eur. J. Phys. **23**, 11 (2002).
[28] J. Tersoff and D. R. Hamann, Phys. Rev. Lett. **50**, 1998 (1983); Phys. Rev. B **31**, 805 (1985).
[29] In Ref. 10, it was reported that P_1 is located at 0.1 eV below the edge of the valence band and P_2 is located at 0.2 eV above the edge of the conduction band. Here, the band gap was measured to be 0.5 eV.
[30] We assume that at room temperature the C defect favors the NM configuration over the AF one because of an enhanced entropy contribution to the free energy.
[31] J. Dabrowski and M. Scheffler, Appl. Surf. Sci. **56-58**, 15 (1992).